RSC Advances

PAPER

View Article Online
View Journal | View Issue

Cite this: *RSC Adv.*, 2025, **15**, 25009

Synthesis, characterization, antimicrobial activity and *in silico* study of pyridinium based ionic liquids†

Md. Jahirul Islam,[a] Ashutosh Nath, *[b] Khadiza,[a] Ajoy Kumer,*[de] Prattyasha Barua,[c] Avra Sarkar,[c] Nadia Israt,[c] Minhajul Abedin,[c] Mohammed Majidul Islam[c] and Md. Wahab Khan*[ae]

Received 23rd May 2025
Accepted 9th July 2025

DOI: 10.1039/d5ra03648h

rsc.li/rsc-advances

A series of twenty-one pyridinium-based ionic liquids (ILs) was synthesized and thoroughly characterized using FTIR, NMR, UV-Vis spectroscopy, and melting point analysis. The ILs' antibacterial activity was assessed against *Aspergillus niger* and a panel of bacteria, both Gram-positive and Gram-negative. Notable antibacterial and antifungal properties were demonstrated by **IL-10**, **IL-11**, and **IL-14** specifically. Several ILs also demonstrated effective Brønsted acidic catalysis for the Mannich process under mild, solvent-free circumstances. The biological activity of **IL-19** and **IL-21** was found to be correlated with their significant binding affinities to microbial protein targets, as demonstrated by molecular docking experiments. Selected ILs, especially **IL-05** and **IL-21**, were found to be drug-like and biosafe based on ADMET and toxicity predictions. These results highlight the pyridinium-based ILs' multipurpose potential as green catalysts and antibacterial agents for sustainable synthetic applications.

1. Introduction

In recent years, there has been increased interest in the unique and remarkable properties of ionic liquids (ILs), including their strong electrical conductivity, low vapor pressure, non-volatility, non-flammability, and improved thermal stability.[1–3] This is attributed to numerous combinations of cations and anions that meet the definition of ILs, leading to adverse suite of behaviors.[4] ILs are normally defined as compounds completely composed of ions with melting points below 100 °C.[5,6] An ionic liquid (IL) is a liquid containing ions *i.e.* organic/inorganic cations and anions (Fig. 1). Although in some papers, ionic liquids are referred as 'molten salts', there is an arbitrary distinction between molten salts and ionic liquids.[7,8]

The first IL (ethyl ammonium nitrate) was reported by Paul Walden in 1914, who at that time never imagined that ILs would become a major scientific area after almost a century. Actually, ILs as innovative fluids have received wide attention only during the past two decades.[9,10] Nowadays more and more researchers are engaged in studying this exciting area, with the outcomes being plentiful.[11–13] A multidisciplinary study on ILs is emerging, including chemistry, materials science, chemical engineering and environmental science.[14,15] More specifically, some important fundamental viewpoints are now different from the original concepts, as insights into the nature of ILs become deeper.[16] Besides, it was opened a new window for drug discovery in pharmaceutics and medicine as bioactive molecules of anti-cancer, antimicrobial agents, anti-viral, antifungal and antiparasitic drugs, anti-infective defense, as well as in the pharmaceutical and food industries, agro-chemistry, artificial enzymes biocides and biotechnology.[17,18] The environmentally benign nature of many ionic liquids further underscores their appeal, offering sustainable alternatives to conventional solvents laden with environmental and health hazards (Fig. 2).[19,20]

In this study, we synthesized a new series of twenty-one pyridinium based ILs and their physicochemical properties were studied by computational approach. Our goal is to identify the ionic liquids by their toxicological analysis, antimicrobial activity and catalytic effects.

2. Experimental

2.1. General method of ILs synthesis

Pyridinium-based ionic liquids (ILs) were produced through the neutralization reaction of pyridine or its derivatives with carboxylic acid in Scheme 1. The initial step involved dissolving the solid base by stirring in ethyl acetate solvent followed by the

[a]*Department of Chemistry, Bangladesh University of Engineering and Technology (BUET), Dhaka, Bangladesh*

[b]*Department of Chemistry, University of Massachusetts Boston, MA 02125, USA. E-mail: ashutosh.nath001@umb.edu*

[c]*Department of Chemistry, Govt. Hazi Muhammad Mohsin College Chattogram, Chattogram, Bangladesh*

[d]*Center for Global Health Research, Saveetha Medical College and Hospitals, Saveetha Institute of Medical and Technical Sciences, Chennai-602105, Tamil Nadu, India*

[e]*Department of Chemistry, International University of Business Agriculture and Technology (IUBAT), Dhaka, Bangladesh*

† Electronic supplementary information (ESI) available. See DOI: https://doi.org/10.1039/d5ra03648h

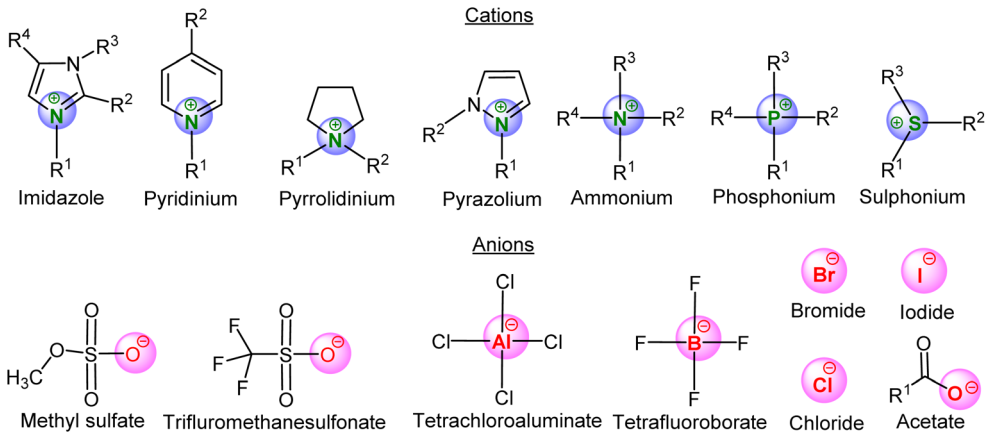

Fig. 1 Commonly used cations and anions in ionic liquids.

gradual addition of acid using a pipette. Due to endothermic reaction, after adding acid to control the thermal output of the procedure, an ice bath was utilized, and nitrogen gas was employed to create an inert atmosphere. The stirring remained consistently for a duration of 6–12 hours, and even up to 30 hours, while the reaction was monitored through thin layer chromatography (TLC) using the aluminum sheet coated with silica gel with MeOH : $CHCl_3$ (30 : 70) as a mobile phase that shows the formation of expected product spot in UV lamp (254 nm). Additionally, for improving the yield, the reaction mixture was heated for 2–3 hours with paraffin oil bath at 50–55 °C temperature. Then the solvent was removed by rotary evaporator and obtained colored or colorless ILs. For further purification it was kept in vacuum oven at 90 °C for two days. The synthesis of the 21 ionic liquids (ILs) was achieved through the utilization of equimolar quantities of organic acids combined with pyridine or its derivatives.

2.2. Instrumental analysis and characterizations of ILs

The synthesized ILs are characterized by using Spectroscopy Infrared (IR) and Nuclear Magnetic Resonance (NMR). The purity of synthesized ILs were maintained using vacuum oven and desiccators throughout the experimental period. The infrared (FT-IR) spectra of synthesized ILs are obtained on a Shimadzu Fourier-Transform Infrared spectrometer (Shimadzu IR Prestige 21, Shimadzu Corporation). The ILs solid samples were mixed with dry KBr to make a thin plate for IR record. For liquid samples, a blank KBr disc is swapped with a small amount of ILs and put in the hole in a radiation chamber. The FT-IR spectra produced had a wave number range of 600–4000 cm^{-1}. In NMR, 5 to 10 mg of sample was dissolved

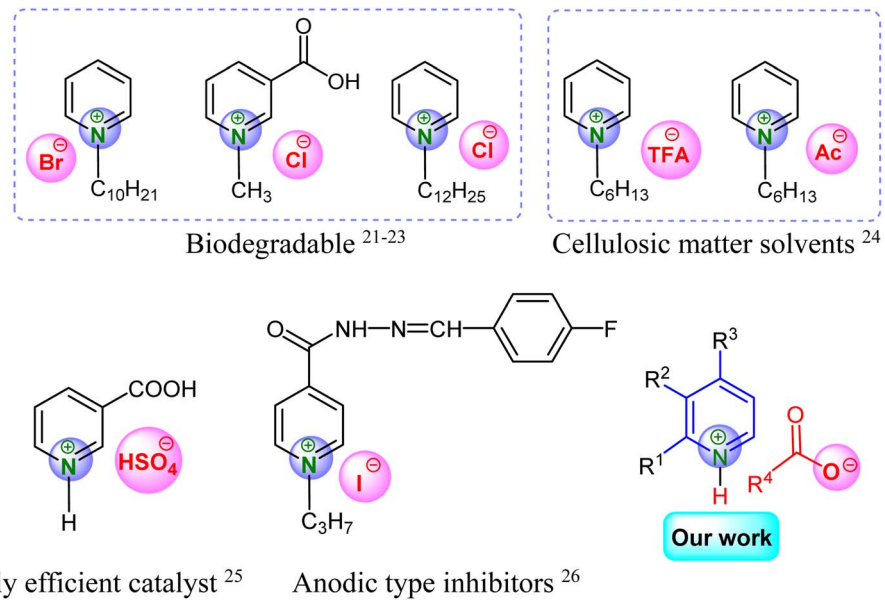

Fig. 2 Some pyridinium containing ILs, With their low volatility and potential for recycling, ionic liquids present promising opportunities for greener synthesis routes and cleaner processes, aligning with the growing imperative for eco-friendly practices in both academic research and industrial applications.[21–28]

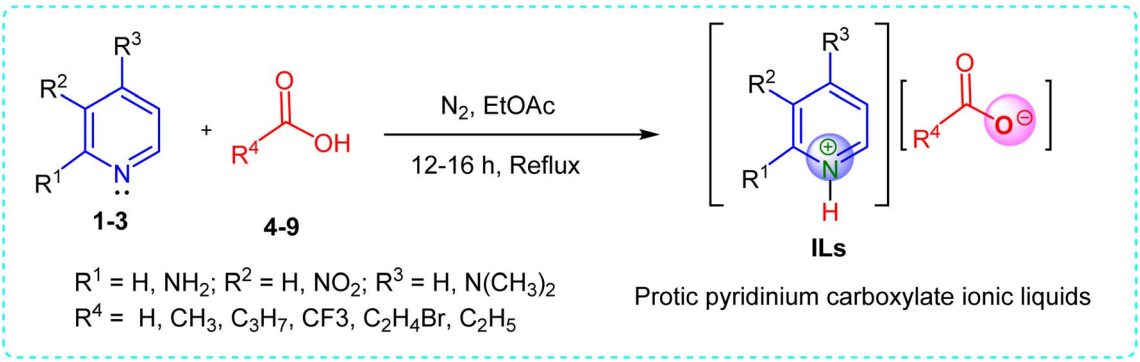

Scheme 1 Synthesis of pyridinium carboxylate ionic liquids.

in 0.7 mL of suitable solvent ($CDCl_3$, CD_3OD). The ^1H NMR spectra were recorded at room temperature on Bruker Avance 400 MHz spectrometer.

2.2.1. Pyridinium trifluoroacetate (IL-05). [C_5H_5N] [C_2F_3-OOH]. M.W.: 193.12 g. M.P.: 84–86 °C. Yield (%): 95%. Physical state: colorless liquid. UV (λ): 255.0 nm. FT-IR (KBr) in cm^{-1}: 3442.3 (–NH); 3096, 2986 (–C–H); 1674 (C═O); 1556 (C═C); 1134 (–C–O); 758,722 (C–H). ^1H NMR chemical shifts: 7.90 (q, 2H, C-3,5); 8.40 (t, 1H, C-4); 8.87 (d, 2H, C-2,6); 13.96 (s, 1H, NH1).

2.2.2. Pyridinium 2-bromopropionate (IL-06). [C_5H_5N] [C_2-$H_4BrCOOH$]. M.W.: 232.07 g. M.P.: 16–18 °C. Yield (%): 93%. Physical state: colorless liquid. UV (λ): 252.0 nm. FT-IR (KBr) in cm^{-1}: 3436 (–NH); 3096 (–C–H); 2959 (–CH_3); 1774 (C═O); 1633 (C═C); 1186 (–C–O); 860 (C–H). ^1H NMR chemical shifts: 1.86 (d, 3H, C-7); 4.38 (q, 1H, C-8); 5.50 (m, 1H, NH1); 8.02 (m, 2H, C-3,5); 8.51 (m, 1H, C-4); 8.86 (d, 2H, C-2,6).

2.2.3. 4-Dimethyl-amino-pyridinium trifluoroacetate (IL-11). [$C_7H_{10}N_2$] [C_2F_3OOH]. M.W.: 236.19 g. M.P.: 156–158 °C. Yield (%): 92%. Physical state: white solid crystal. UV(λ): 286.0 nm. FT-IR (KBr) in cm^{-1}: 3455 (–NH); 3077 (–C–H); 2959 (N–CH_3); 1888 (C═O); 1649 (C═C); 1202 (–CH_3); 1188 (–C–O); 1138 (C–F); 860, 718 (C–H). ^1H NMR chemical shifts: 3.22 (s, 2H, NC-4); 6.76 (t, 2H, C-3,5); 8.18 (t, 2H, C-2,6); 13.28 (s, 1H, NH1).

2.2.4. 4-Dimethyl-amino-pyridinium 2-bromo propionate (IL-12). [$C_7H_{10}N_2$] [$C_2H_4BrCOOH$]. M.W.: 275.14 g. M.P.: 50–52 °C. Yield (%): 94%. Physical state: white solid crystal. UV(λ): 285.0 nm. FT-IR (KBr) in cm^{-1}: 3494 (–NH); 3078 (–C–H); 2908 (–CH_3); 1739 (C═O); 1648 (C═C); 1209 (–CH_3); 1148 (–C–O); 1138 (C–F); 860, 798 (C–H). ^1H NMR chemical shifts: 3.10 (d, 3H, C-8); 4.38 (q, 1H, C-8); 4.70 (s, 6H, NC-4); 6.75 (d, 2H, C-3,5); 7.96 (d, 2H, C-2,6); 13.30 (s, 1H, NH1).

2.2.5. 2-Amino-3-nitro pyridinium trifluoroacetate (IL-17). [$C_5H_5N_3O_2$] [C_2F_3OOH]. M.W.: 253.13 g. M.P.: 97–99 °C. Yield (%): 91%. Physical state: yellowish white solid crystal. UV(λ): 389.0 nm. FT-IR (KBr) in cm^{-1}: 3466 (–NH); 3362, 3356 (–NH_2); 3096 (–C–H); 2924 (CH); 2372 (–NO_2); 1702 (C═O); 1568 (C═C); 1202 (–CH_3); 1142 (–C–O); 1096 (C–F); 805, 628 (C–H). ^1H NMR chemical shifts: 5.85 (s, 1H, NH1); 6.81 (q, 1H, C-4); 7.28 (s, 2H, NH2); 8.36 (d, 1H, C-3); 8.53 (d, 1H, C-2).

2.2.6. 2-Amino-3-nitro pyridinium 2-bromopropionate (IL-18). [$C_5H_5N_3O_2$] [$C_2H_4BrCOOH$]. M.W.: 292.08 g. M.P.: (−5–4) °C. Yield (%): 91%. Physical state: reddish liquid. UV(λ): 389.0 nm. FT-IR (KBr) in cm^{-1}: 3446 (–NH); 3362, 3356 (–NH_2); 3096 (–C–H); 2924 (C–H) (–CH_3); 2372 (–NO_2); 1702 (C═O); 1568 (C═C); 1202 (–CH_3); 1142 (–C–O); 1096 (C–F); 805, 628 (C–H). ^1H NMR chemical shifts: 1.90 (d, 3H, C-5); 4.42 (m, 1H, C-6); 7.70 (s, 1H, NH1); 6.83 (q, 1H, C-4); 7.88 (s, 2H, NH2); 8.30 (d, 1H, C3); 8.60 (d, 1H, C-2).

2.2.7. Benzyl pyridinium chloride (IL-19). [C_5H_5N] [C_7H_7Cl]. M.W.: 205.69 g. M.P.: 12–14 °C. Yield (%): 97%. Physical state: colorless liquid. UV (λ): 258.0 nm. FT-IR (KBr) in cm^{-1}: 3050: (–C–H); 2969 (C–H); 2864 (–CH_2); 1660 (C═C); 1207 (–CH_2); 1159 (–C–O); 1027 (N–Cl); 748, 628 (C–H). ^1H NMR chemical shifts: 6.34 (s, 2H, C-7); 7.36 (t, 3H, C 9–11); 7.69 (t, 2H, C-8,12); 8.02 (t, 2H, C-3,5); 8.38 (t, 1H, C-4); 9.66 (d, 2H, C-2,6).

2.2.8. 2-(Phenyl(m-tolylamino)methyl)cyclohexan-1-one 13. [$C_{20}H_{23}NO$] M.W.: 294.84 g. M.P.: 136–138 °C. Yield (%): 97%. Physical state: white solid crystal. UV(λ): 261.0 nm. FT-IR (KBr) in cm^{-1}: 3387.11 (–NH); 3037.99 (–C–H); 2947 (–CH_2); 2913 (–CH); 1701 (–CO–); 1595 (C═C); 1207 (–CH_2); 1120 (–C–O); 748, 705 (C–H). ^1H NMR chemical shifts: 1.90 (m, 4H, C-3,4); 1.74 (m, 2H, C-5); 2.23 (s, 3H, C-10); 2.48 (t, 2H, C-6); 2.84 (t, 1H, C-7); 4.64 (d, 1H, C-8); 4.84 (d, 1H, C-2); 6.44 (m, 3H, C11-13); 6.98 (m, 1H, C9); 7.30 (m, 5H, C14–18).

2.3. Computational procedure

2.3.1. Molecular docking study. The molecular structures (2D, 3D) were cleaned and minimized by Chem3D software which are shown in Table S1A.† Smiles IDs of ionic liquids (ILs) were identified by using ChemDraw software, presented in Table S1B.† Through SwissDock software molecular docking was performed where ILs were used as ligands and proteins of bacteria and fungi. The protein files (PDB) were collected from the RCSB protein data bank and prepared by using Discovery Studio 2021.[29] The molecular docking was completed by the method of Autodock Vina[30] from SwissDock.[31] ADMET data and druglike nature properties are taken from online servers: ADMETSAR and SWISSADME to calculate ADMET (Absorption, Distribution, Metabolism, Excretion and Toxicity) parameters.[32]

2.3.2. ADMET study. ADMET data and druglike nature properties are taken from online servers: ADMETSAR and SWISSADME to calculate ADMET (Absorption, Distribution, Metabolism, Excretion and Toxicity) parameters.[33] Toxicity data

Table 1 Catalytic properties of ILs in Mannich reaction

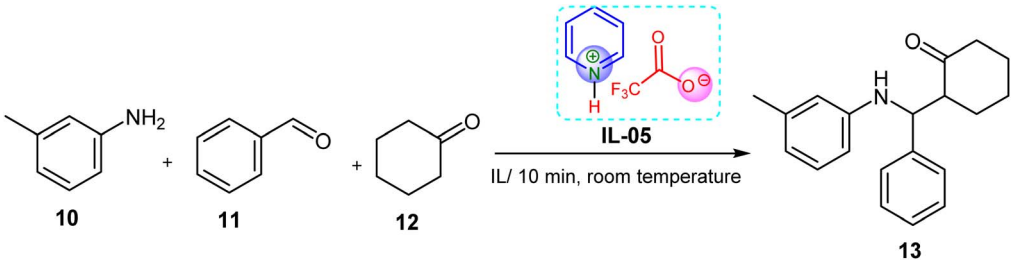

ILs	Amount (wt%)	Time (min)	Yield[a] (%)
IL-05	18.69	10	91
IL-05	**21.49**	**10**	**96.7**
IL-11	21.49	30	85
IL-17	23.36	20	93

[a] Reaction condition: **10 : 11 : 12** (1 : 1 : 1) mole ratio; temperature at 25 °C; two drops of water (0.06 g) were added into ionic liquid to allow proper mixing.

is collected and analysed by using the SMILES ID of twenty-one ILs. Biodegradability results of these PILs were analyzed in Table S7.†

2.4. Biological properties of ILs

Pyridinium-based ionic liquids (ILs) were evaluated for their antibacterial and antifungal properties using standard microbiological techniques. ILs were prepared in concentrations ranging from 1000 mM to 50 mM *via* serial dilution. Antibacterial activity was assessed against six human pathogens (Gram-positive and Gram-negative) using the well diffusion method on nutrient agar. Zones of inhibition were measured, and minimal inhibitory concentrations (MICs) were determined for active compounds. Antifungal activity was tested against *Aspergillus niger* and *Rhizopus azzahra* using potato dextrose broth medium and well diffusion method. The influence of IL concentration, anionic structure, and functional groups on antimicrobial activity was systematically analyzed. More details of antibacterial working procedure in ESI.†

2.5. Investigation of catalytic properties of ILs

In a typical reaction, a mixture of benzaldehyde (1 mmol), 3-methylaniline (1 mmol), cyclohexanone (1.1 mmol), and synthesized ionic liquid (0.20–0.25 g) was stirred at room temperature (25 °C) in a round-bottom flask. Two drops of water (~0.06 g) were added to facilitate homogenization. The reaction mixture gradually became viscous and solidified. The resulting solid was isolated by filtration, washed, and recrystallized from 98% ethanol. The final product was dried under reduced pressure using a Hoover pump for 5 hours. Reaction yields and times were summarized in Table 1. The products were characterized by ^{1}H NMR and FT-IR spectroscopy.

3. Result and discussion

3.1. Catalytic properties of ILs

In a standard reaction, a solution containing 1 mmol of benzaldehyde **11**, 1 mmol of 3-methylaniline **10**, 1.1 mmol of cyclohexanone **12**, and 18.69 wt% (20 g, based on cyclohexanone) of ionic liquids as catalysts and solvent was prepared by mixing them in a round-bottomed flask at the ambient temperature of 25 °C. The mixture of the reaction became viscous and solidified. The solid was segregated through the process of filtration, and subsequently, the resulting product **13** underwent recrystallization from 98% ethanol and was subjected to hoover drying for a duration of 5 hours. Table 1 is presents a summary of the results obtained from the Mannich reaction involving aldehydes, ketones, and amines. This reaction takes place under the influence of Brønsted acidic ionic liquids and is typically carried out at ambient temperature. Room temperature, a small amount of ionic liquid can facilitate this single-step reaction involving aldehydes, amines, and ketones, known as the Mannich type reaction. The identification of the compound was accomplished by employing ^{1}H NMR and as well as FT-IR.

In comparison, **IL-11** required a longer reaction time of 30 minutes and resulted in a lower yield (85%), suggesting lower catalytic activity. **IL-17** performed moderately, offering a 93% yield in 20 minutes with 23.36 wt% of catalyst. These findings highlight **IL-05** (21.49 wt%) as the most effective and rapid catalyst, capable of significantly enhancing product 96.7% yield in minimal time, thereby confirming its promising application in green and efficient Mannich-type transformations under mild conditions.

In contrast, 4-dimethylaminopyridinium trifluoroacetate (**IL-11**) showed comparatively lower activity, providing a yield of 85% over 30 minutes, despite being used at the same concentration. The reduced efficiency of **IL-11** may be attributed to the

Table 2 Data of zone of inhibition for antibacterial activity

Ionic liquids	*Bacillus cereus* (+)	*Staphylococcus aureus* (+)	*Sarcina lutea* (+)	*Salmonella typhi* (−)	*Escherichia coli* (−)	*Pseudomonas aeruginosa* (−)
IL-01	0	0	19 ± 1	0	32 ± 1	30 ± 1
IL-02	0	0	24 ± 1	0	0	22 ± 1
IL-03	0	19 ± 1	20 ± 1	0	0	28 ± 1
IL-04	0	0	0	0	27 ± 1	0
IL-05	0	0	0	0	25 ± 1	0
IL-06	18 ± 1	16 ± 1	22 ± 1	15 ± 1	27 ± 1	21 ± 1
IL-07	20 ± 1	19 ± 1	20 ± 1	28 ± 1	30 ± 1	26 ± 1
IL-08	16 ± 1	22 ± 1	21 ± 1	24 ± 1	25 ± 1	21 ± 1
IL-09	22 ± 1	20 ± 1	18 ± 1	24 ± 1	20 ± 1	25 ± 1
IL-10	30 ± 1	35 ± 1	31 ± 1	36 ± 1	33 ± 1	31 ± 1
IL-11	28 ± 1	26 ± 1	31 ± 1	30 ± 1	32 ± 1	26 ± 1
IL-12	24 ± 1	22 ± 1	20 ± 1	28 ± 1	28 ± 1	25 ± 1
IL-13	18 ± 1	19 ± 1	21 ± 1	24 ± 1	28 ± 1	25 ± 1
IL-14	23 ± 1	17 ± 1	16 ± 1	24 ± 1	25 ± 1	28 ± 1
IL-15	18 ± 1	16 ± 1	17 ± 1	18 ± 1	23 ± 1	21 ± 1
IL-16	19 ± 1	15 ± 1	14 ± 1	16 ± 1	15 ± 1	21 ± 1
IL-17	20 ± 1	24 ± 1	22 ± 1	24 ± 1	23 ± 1	26 ± 1
IL-18	22 ± 1	21 ± 1	24 ± 1	18 ± 1	25 ± 1	23 ± 1
IL-19	09 ± 1	18 ± 1	19 ± 1	24 ± 1	23 ± 1	24 ± 1
IL-20	18 ± 1	19 ± 1	17 ± 1	23 ± 1	18 ± 1	20 ± 1
IL-21	20 ± 1	18 ± 1	17 ± 1	35 ± 1	30 ± 1	28 ± 1

electron-donating dimethylamino substituent, which likely decreases the Brønsted acidity of the ionic liquid, thereby diminishing its catalytic performance.

The products obtained were characterized and confirmed by ^{1}H NMR and FT-IR spectroscopy. These results collectively demonstrate that the catalytic efficiency of pyridinium-based ILs is significantly influenced by their electronic structure,

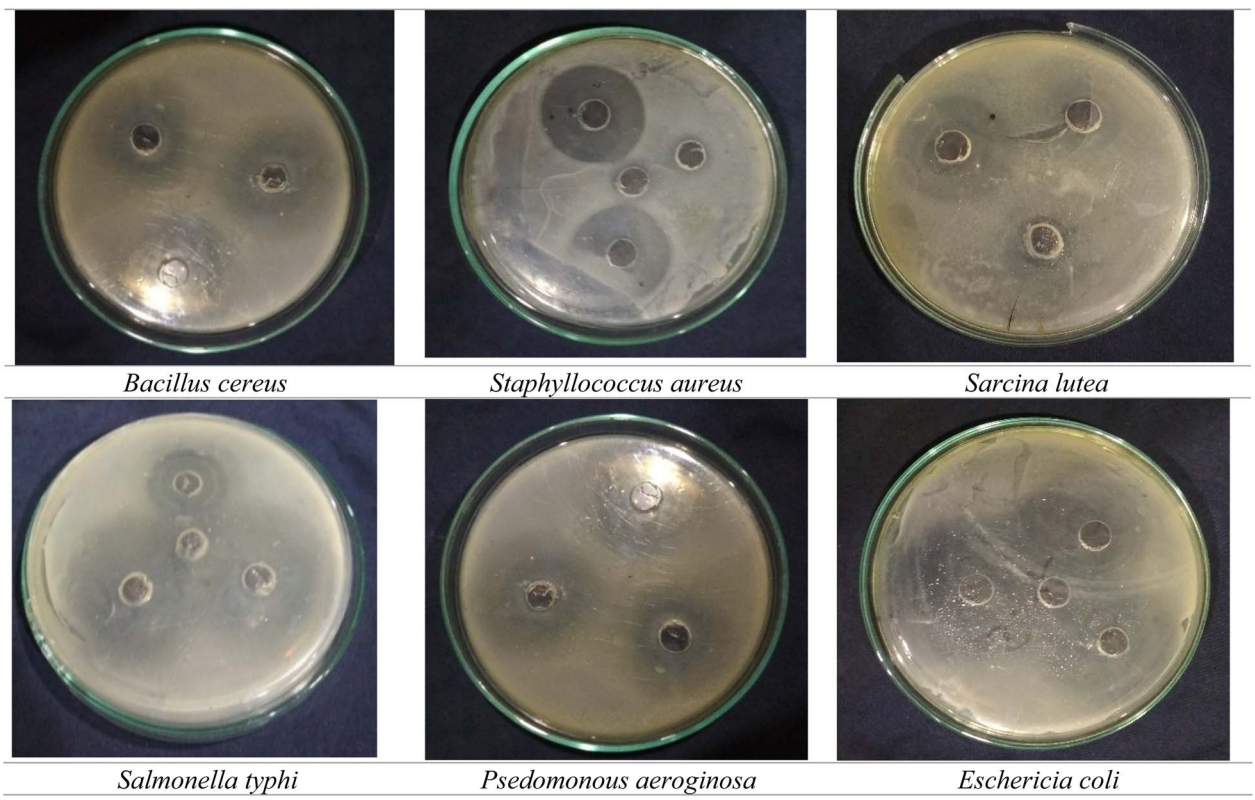

Fig. 3 Six human pathogens Gram positive and Gram negative which were killed by different types of pyridinium based ionic liquids.

with **IL-05** emerging as the more effective catalyst for Mannich-type transformations under mild, solvent-assisted conditions.

3.2. Biological properties of ILs

3.2.1. Antibacterial studies. Subtracting the well diameter 5.0 mm, the bacterial inhibition zone of six Gram positive and Gram-negative pathogens were measured by using well diffusion method in mm for 1000, 500 and 100 mM for pyridinium based twenty-one synthesized IL's. The values are recorded in Table 1. According to Table 2 and Fig. 3, **IL-10** ranked first position by value for all pathogens while the value is highest for *Salmonella typhi* with the result of 36 mm. It was noticed that *Escherichia coli* pathogenic bacteria were procured as $-CH_3$ > $-NO_2$ > –OH > Pyridine. Besides, Nitro group increased toxicity among all pathogenic bacteria except *Escherichia coli*.

The antimicrobial screening of 21 from Table 2 synthesized ILs against Gram-positive (*Bacillus cereus*, *Staphylococcus aureus*, *Sarcina lutea*) and Gram-negative (*Salmonella typhi*, *Escherichia coli*, *Pseudomonas aeruginosa*) bacteria showed significant variation in activity depending on IL structure and bacterial strain. **IL-10**, **IL-11**, and **IL-21** exhibited strong, broad-spectrum activity with inhibition zones of 26–36 ± 1 mm across all tested bacteria. In contrast, **IL-01**, **IL-02**, **IL-04**, and **IL-05** showed limited activity against Gram-positive strains but moderate to high efficacy against *E. coli* and *P. aeruginosa*. **IL-06** through **IL-09** and **IL-12** through **IL-20** demonstrated moderate antimicrobial effects (15–28 ± 1 mm), with some showing greater potency against Gram-negative bacteria, likely due to differences in membrane permeability and ionic interactions. The enhanced activity of ILs such as **IL-10** and **IL-11** may be linked to structural features like electron-donating substituents, aromatic rings, or polar functional groups that facilitate membrane disruption or ionic transport, highlighting important structure–activity relationships.

3.2.2. Antifungal activity. Antifungal analysis can be determined by the term growth percentage with the control of 100%. The growth percentage is deducted as the following questions.

$$\%\ \text{Growth} = \frac{\text{Growth of fungi without IL's solution as control}}{\text{Growth of fungi with IL's solution}} \times 100\%$$

Activity of antifungal can be considered as a term inversely with growth percentage called inhibition percentage. Subtracting the growth percentage from control, inhibition percentage can be calculated.

From the listed value of inhibition percentage in Table 3, it is evaluated that the effect of the compound is clearly visible. ILs containing 2-amino-3-nitro perform higher antifungal activity. Though all the compounds showed antifungal activity, the rate is dependent on different groups of compounds. Among all, 2-amino-3-nitro pyridinium based ILs perform comparatively higher antifungal activity. **IL-14** has the lowest growth zone that indicates the highest inhibition percentage and the lowest antifungal activity for the fungi.

Table 3 Zone of growth observed from the antifungal test (*Aspergillus niger*)

Chemicals tested	Zone of growth	Percent of growth
Control	28 mm	100%
IL-01	20.5 ± 1	78.57%
IL-02	19.0 ± 1	67.80%
IL-03	25.0 ± 1	89.28%
IL-04	14.5 ± 1	51.78%
IL-05	12.5 ± 1	46.67%
IL-06	25.5 ± 1	91.07%
IL-07	22.0 ± 1	78.85%
IL-08	18.0 ± 1	64.28%
IL-09	17.0 ± 1	60.71%
IL-10	23.0 ± 1	82.14%
IL-11	18.5 ± 1	64.28%
IL-12	27.0 ± 1	96.62%
IL-13	25.0 ± 1	89.28%
IL-14	5.0 ± 1	17.85%
IL-15	12.7 ± 1	45.53%
IL-16	14.8 ± 1	52.75%
IL-17	22.7 ± 1	81.25%
IL-18	26.5 ± 1	92.85%
IL-19	15.5 ± 1	53.35%
IL-20	18.5 ± 1	66.07%
IL-21	26.2 ± 1	93.75%

The antimicrobial efficacy of the synthesized ILs was quantitatively assessed by measuring the zone of growth inhibition and calculating the corresponding percent growth relative to the control. The control showed a zone of growth of 28 ± 1 mm, representing 100% bacterial growth. Among the ILs, **IL-12** (27.0 ± 1 mm, 96.62%), **IL-18** (26.5 ± 1 mm, 92.85%), and **IL-21** (26.2 ± 1 mm, 93.75%) showed the least inhibition of bacterial growth, indicating relatively low antimicrobial activity. Conversely, **IL-14** demonstrated the strongest inhibitory effect with only 5.0 ± 1 mm zone of growth and 17.85% growth, suggesting high antimicrobial potency. Other ILs such as **IL-05** (12.5 ± 1 mm, 46.67%), **IL-04** (14.5 ± 1 mm, 51.78%), and **IL-15** (12.7 ± 1 mm, 45.53%) also exhibited significant bacterial growth suppression. Moderate inhibitory effects were observed in **IL-01**, **IL-02**, **IL-08**, and **IL-11** with zones of growth between 18.0–20.5 ± 1 mm, corresponding to 64–79% growth. The variation in antimicrobial performance among ILs suggests that their chemical structure influences their ability to inhibit bacterial proliferation. ILs with lower percent growth values demonstrate stronger antimicrobial action, which could be due to enhanced membrane disruption or interference with bacterial metabolism.

3.3. *In silico* study of ILs

3.3.1. Molecular docking. The chosen proteins are crucial enzymes or structural elements in bacteria and fungus, rendering them pertinent targets for antibacterial strategies. Docking experiments on these proteins evaluates the binding affinity and inhibitory efficacy of the produced ionic liquids. The docking study has been applied to find out the interaction between ILs (ligands) and proteins (macromolecules) of six

Table 4 Molecular docking score using AutoDock Vina

	Binding affinity (kcal mol^{-1})						
Ionic liquids	*Aspergillus niger* (2BJH)	*Bacillus cereus* (+) (1QS1)	*Escherichia coli* (−) (1JG0)	*Pseudomonas aeruginosa* (−) (4ESH)	*Salmonella typhi* (−) (1 A5A)	*Sarcina lutea* (+) (1GWF)	*Staphylococcus aureus* (+) (4CJN)
IL-06	−3.98	−4.28	−4.15	−4.54	−4.08	−4.31	−3.80
IL-09	−4.86	−5.08	−4.61	−4.99	−4.56	−5.15	−4.03
IL-10	−4.82	−5.08	−4.61	−4.99	−4.56	−5.12	−4.15
IL-15	−5.39	−6.14	−5.32	−5.92	−5.39	−5.50	−4.85
IL-16	−5.39	−6.14	−5.33	−5.91	−5.42	−5.46	−4.85
IL-19	−6.09	−7.14	−5.51	−6.81	−6.42	−7.29	−5.79
IL-21	−6.06	−7.01	−5.53	−6.72	−6.41	−6.32	−5.09

bacteria's and one fungus, such as: *Bacillus cereus* (+), *Staphylococcus aureus* (+), *Sarcina lutea* (+), *Salmonella typhi* (−), *Escherichia coli* (−), *Pseudomonas aeruginosa* (−) and *Aspergillus niger*. Docking scores of pathogens with ILs are shown in Table 4. The binding affinity with − 6.0 kcal mol^{-1} or higher score of pathogens indicates as the standard drugs. Among all, the score was too low with the starting ILs but benzyl pyridinium based ILs showed the best results.

IL-06 topped among the pyridinium groups whereas **IL-09** and **IL-10** showed the highest scores in the 4-dimethyl amino pyridinium group. On the other hand, **IL-16** had the best result in the 2-Amino-3-nitro pyridinium group. Lastly, **IL-19** and **IL-21** had the highest binding affinity in the benzyl pyridinium group as well as among the total twenty-one ionic liquids (IL). All of the ILs' docking scores are shown in Table S5.† The parameters

Table 5 *In vivo* predicted LD_{50} toxicity profiles of synthesized ILs (1–21)

Compound	AMES toxicity	Carcinogenicity	Acute Oral Toxicity [b]
IL-01			IV
IL-02			III
IL-03			III
IL-04			III
IL-05			III
IL-06			III
IL-07			II
IL-08			II
IL-09			II
IL-10			III
IL-11			III
IL-12			III
IL-13			III
IL-14			III
IL-15			III
IL-16			III
IL-17			III
IL-18			III
IL-19			III
IL-20			III
IL-21			III

: Non-Toxic; : Toxic : Non-Carcinogens

[b] [Based on the criterion of US EPA, the acute oral toxicity is classified in four categories based on LD_{50} values. Category I = Highly toxic; Category II = Moderately toxic; Category III = Slightly toxic; Category IV = Practically non-toxic].

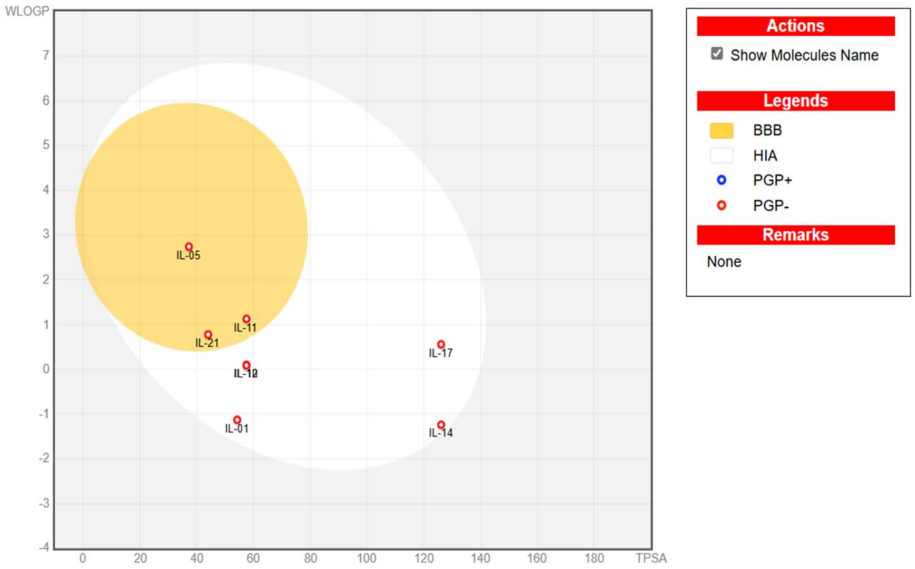

Fig. 4 Boiled egg representation of ILs.

(Grid box value) for all seven proteins (PDB) are mentioned in Table S5A.†

3.3.2. ADMET study. ADMET study plays a dominant role in drug discovery. ADMET is an abbreviation of Absorption, Distribution, Metabolism, Excretion and Toxicity. The ADMET table illustrates that all ILs abide by the Lipinski rule which means they show zero violation that also indicates good binding affinity. In this article, human intestinal absorption, blood–brain barrier, renal organic transporter, Caco-2 permeability, P-1 glycoprotein Inhibitor, P-2 glycoprotein substrate, CYP450 1A2 inhibitor, CYP450 2C9 substrate and Sub-Cellular localization are studied for all of the twenty-one ILs. Table S6† contains the data of *In silico* pharmacokinetic predictions of ILs.[34,35]

3.3.3. *In silico* analysis. Clinical trials eligibility requires completion of silico pharmacokinetic and bioavailability studies. This has led to the performance of pharmacokinetic and bioavailability studies, the outcomes of which are mentioned in Table S6.† Human intestinal absorption is positive in case of all ILs. According to Table S6,† **IL-05**, **IL-11**, **IL-20** and **IL-21** showed positive results for BBB. The rest of the ILs can't cross the blood–brain barrier. All of the ILs are non-inhibitors. These ILs are non-inhibitors in the case of Renal organic cation transporters. IL-(05, 13, 14, 15, 16, 17, 18, 19) and **IL-20** are CYP450 1A2 inhibitors and the rest of the ILs are non-inhibitors. CYP450 2C9 substrate refers to a drug or chemical that will undergo a chemical or metabolic reaction with the CYP450 2C9 enzyme to produce products or metabolites that are different from the original substrate. These ILs are negative, which means ILs do not undergo any reaction with the CYP450 2C9 enzyme. Subcellular localization of these ILs is in mitochondria.[29,36]

3.3.4. Physicochemical properties. Any medicine and its efficacy as a leading contender against any illness must pass *In silico* physiochemical analysis, or ADMET. Physicochemical

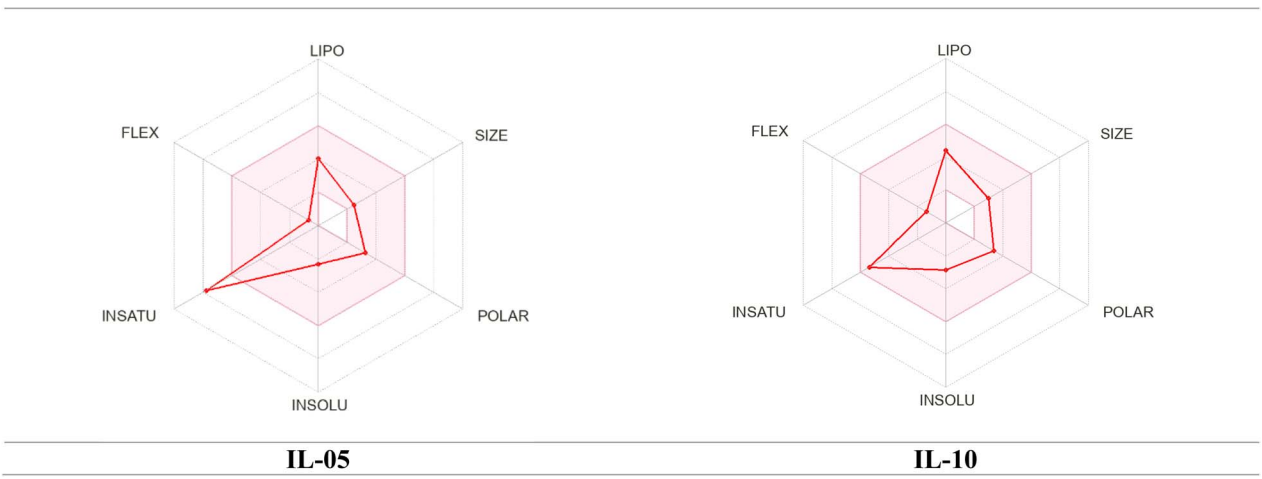

Fig. 5 Bioavailability radar of ILs.

properties of these 21 ILs are formed in Table S7.† Oral bioavailability requires the topological polar surface (TPSA to be ≤ 140 Å^2). All of the ILs showed good oral bioavailability (TPSA range = 3.88–126.11).

3.3.5. Analysis of toxicity. Table 5 and Table S8† predict the toxicity profile of synthesized ILs 01–21. High solubilities cause water pollution. IL05, IL10, IL15 are less soluble. Acute oral toxicity was found in four categories. Oral rat acute toxicity, fish toxicity and *T. pyriformis* show medium affinity.

According to toxicity data, all ILs are non-carcinogenic. ADMET toxicity was accomplished and **IL-13** to **IL-20** tested positive. Based on *In vivo* antibacterial activity and estimated LD_{50} levels in rat acute toxicity studies, the drugs appear to be safe (1.6339–2.7181 mol kg^{-1}).

3.3.6. Boiled egg model. The BOILED-Egg method confidently models the permeation of curcumin and Schiff base diol monomers. The boiled egg technique is commonly used to evaluate passive gastrointestinal absorption (HIA) and brain penetration (BBB) in relation to the comparison between *W* LOG *P* and TPSA.[37] The white yolk of the egg demonstrates a significant likelihood of being passively absorbed by the gastrointestinal tract, whereas the yellow region (yolk) exhibits a high probability of penetrating the brain. Fig. 4 shows that **IL-05**, **IL-11** and **IL-21** are in the yellow region while **IL-01**, **IL-10**, **IL-14** and **IL-17** are in the white part (Fig. 5).

The bioavailability radar visualizes the drug-likeness and pharmacokinetic properties of an ionic liquid. The lipophilicity (Log *P*) indicates the solubility of an IL in fats *vs.* water. Bioavailability radar of twenty-one ILs is shown in Table S9.†

4. Conclusion

This study used FTIR, NMR, and UV-Vis techniques to successfully synthesize and analyze 21 pyridinium-based ionic liquids (ILs). The synthesized ionic liquids (ILs) were successfully prepared with high purity and yields (91–97%) and characterized by FT-IR and ^{1}H NMR, confirming their structural integrity. UV-Vis data supported aromatic features, and defined melting points indicated reproducible synthesis. These ILs hold promises for further applications due to their distinct structural and electronic properties. In mild conditions, several ILs also functioned as efficient catalysts in the Mannich process. The study shows that several synthesized ILs exhibit notable antimicrobial activity. **IL-10**, **IL-11**, and **IL-21** are effective broad-spectrum agents, while **IL-01** and **IL-05** selectively target Gram-negative bacteria. Some ILs like **IL-14**, **IL-05**, and **IL-04** strongly inhibit bacterial growth, whereas **IL-12**, **IL-18**, and **IL-21** are less effective. These results highlight the role of structural features in antimicrobial efficacy and support further research into their mechanisms and therapeutic potential. Their antibacterial potential was supported by molecular docking, which showed that **IL-19** and **IL-21** had favorable binding affinities against bacterial and fungal proteins. For important ILs like **IL-05** and **IL-21**, ADMET and toxicology tests verified good drug-like qualities and minimal toxicity. These results imply that pyridinium-based ILs hold promise for use in green catalysis and medication development.

Data availability

The datasets generated and analyzed in this current study are available from the corresponding author upon reasonable request.

Author contributions

JI and AN writing – original draft, review & editing, visualization, software, formal analysis, data curation, software, resources. WK and AK: writing – review & editing, resources, methodology, investigation, supervision. PB, AS, NI, MA, and M: software, methodology, review & editing.

Conflicts of interest

The authors declare that they have no known competing financial interests or personal relationships that could have appeared to influence the work reported in this paper.

Acknowledgements

We are grateful to the Bangladesh University of Engineering and Technology (BUET), Dhaka, Dhaka-1000, Bangladesh for all kinds of experimental and financial supports.

References

1 M. J. Earle, J. M. Esperança, M. A. Gilea, J. N. Canongia Lopes, L. P. Rebelo, J. W. Magee, K. R. Seddon and J. A. Widegren, *Nature*, 2006, **439**, 831–834.
2 J.-Z. Yang and J.-S. Gui, *Acta Chim. Sin.*, 2005, **63**, 577.
3 S. Ahrens, A. Peritz and T. Strassner, *Angew. Chem., Int. Ed. Engl.*, 2009, **48**, 7908–7910.
4 A. Mehrkesh and A. T. Karunanithi, *Fluid Phase Equilib.*, 2016, **427**, 498–503.
5 M. Ahrenberg, M. Beck, C. Neise, O. Keßler, U. Kragl, S. P. Verevkin and C. Schick, *Phys. Chem. Chem. Phys.*, 2016, **18**, 21381–21390.
6 T. Welton, *Biophys. Rev.*, 2018, **10**, 691–706.
7 M. M. Santos, C. Alves, J. Silva, C. Florindo, A. Costa, Ž. Petrovski, I. M. Marrucho, R. Pedrosa and L. C. Branco, *Pharmaceutics*, 2020, **12**, 694.
8 J. Claus, F. O. Sommer and U. Kragl, *Solid State Ionics*, 2018, **314**, 119–128.
9 Z. Zhang, J. Song and B. Han, *Chem. Rev.*, 2017, **117**, 6834–6880.
10 T. Welton, *Chem. Rev.*, 1999, **99**, 2071–2084.
11 A. C. Cole, J. L. Jensen, I. Ntai, K. L. T. Tran, K. J. Weaver, D. C. Forbes and J. H. Davis, *J. Am. Chem. Soc.*, 2002, **124**, 5962–5963.
12 R. D. Rogers and K. R. Seddon, *Science*, 2003, **302**, 792–793.
13 P. G. Jessop, *Faraday Discuss.*, 2018, **206**, 587–601.
14 Z. Lei, B. Chen, Y.-M. Koo and D. R. MacFarlane, *Chem. Rev.*, 2017, **117**, 6633–6635.
15 R. Ferraz, L. C. Branco, C. Prudêncio, J. P. Noronha and Ž. Petrovski, *ChemMedChem*, 2011, **6**, 975–985.

16 R. A. Sheldon, *Green Chem.*, 2007, **9**, 1273–1283.
17 M. I. Hossain and A. Kumer, *Asian J. Chem. Sci.*, 2017, **3**(4), 1–10.
18 W. L. Hough, M. Smiglak, H. Rodríguez, R. P. Swatloski, S. K. Spear, D. T. Daly, J. Pernak, J. E. Grisel, R. D. Carliss and M. D. Soutullo, *New J. Chem.*, 2007, **31**, 1429–1436.
19 A. Hospido and H. Rodríguez, in *Encyclopedia of Ionic Liquids*, Springer, 2023, pp. 813–821.
20 R. F. Frade and C. A. Afonso, *Hum. Exp. Toxicol.*, 2010, **29**, 1038–1054.
21 J. R. Harjani, R. D. Singer, M. T. Garcia and P. J. Scammells, *Green Chem.*, 2009, **11**, 83–90.
22 M. Suk and K. Kümmerer, *Green Chem.*, 2023, **25**, 365–374.
23 M. Trush, L. Metelytsia, I. Semenyuta, L. Kalashnikova, O. Papeykin, I. Venger, O. Tarasyuk, L. Bodachivska, V. Blagodatnyi and S. Rogalsky, *Environ. Sci. Pollut. Res.*, 2019, **26**, 4878–4889.
24 K. Aghmih, H. Wakrim, A. Boukhriss, M. El Bouchti, S. Majid and S. Gmouh, *Polym. Bull.*, 2022, 1–13.
25 A. R. Hajipour and M. Seddighi, *Synth. Commun.*, 2012, **42**, 227–235.
26 F. Hajjaji, R. Salim, M. Taleb, F. Benhiba, N. Rezki, D. Chauhan and M. Quraishi, *J. Taiwan Inst. Chem. Eng.*, 2021, **123**, 346–362.
27 A. H. M. Fauzi and N. A. S. Amin, *Renewable Sustainable Energy Rev.*, 2012, **16**, 5770–5786.
28 J. L. Anderson, D. W. Armstrong and G.-T. Wei, *Anal. Chem.*, 2006, **78**, 2892–2902.
29 S. Sharma, A. Sharma and U. Gupta, *Annals of Antivirals and Antiretrovirals*, 2021, **5**, 028–032.
30 J. Eberhardt, D. Santos-Martins, A. F. Tillack and S. Forli, *J. Chem. Inf. Model.*, 2021, **61**, 3891–3898.
31 M. Bugnon, U. F. Röhrig, M. Goullieux, M. A. Perez, A. Daina, O. Michielin and V. Zoete, *Nucleic Acids Res.*, 2024, **52**, W324–W332.
32 M. Rani, A. Nath and A. Kumer, *J. Biomol. Struct. Dyn.*, 2023, **41**, 8392–8401.
33 A. Daina, O. Michielin and V. Zoete, *Sci. Rep.*, 2017, **7**, 42717.
34 U. A. Çevik, A. Işik and A. Karakaya, *Computational Methods for Rational Drug Design*, 2025, pp. 123–151.
35 J. A. Pradeepkiran, S. Sainath and K. Shrikanya, in *Brucella Melitensis*, Elsevier, 2021, pp. 133–176.
36 M. Marzi, M. K. Vakil, M. Bahmanyar and E. Zarenezhad, *BioMed Res. Int.*, 2022, **2022**, 7341493.
37 A. Daina and V. Zoete, *ChemMedChem*, 2016, **11**, 1117–1121.